# Morphological gradients

Jean-F. Rivest, Pierre Soille and Serge Beucher

Centre de Morphologie Mathématique, Ecole des Mines de Paris
35 rue Saint-Honoré, 77305 Fontainebleau, France

**Abstract**

Object boundaries are generally characterized by grey-level intensity transitions. In order to detect these variations, gradient masks are widely used. In this paper, we survey the morphological framework of gradient operators. Morphological gradients are based on the difference between extensive and anti-extensive transformations. For instance dilations and erosions with structuring elements containing their origin belong to this class of transformations. Generally, these gradients are used in segmentation applications with edge finders such as sequential searches, thresholdings or the watershed transformation. The robustness of this latter transformation allows more tolerance for the construction of a gradient operator. After a short introduction to gradients in digital images we present the gradients available in mathematical morphology: Beucher's gradient, internal and external, thick, regularized, directional, and thinning/thickening gradients. Applicability and performance of each gradient are briefly evaluated. We then generalize the morphological framework of gradient operators to other digital spaces.

# 1 Introduction

Gradient operators are used in segmentation because they enhance intensity variations in images. These variations are assumed to be edges of objects. This is why gradients are also called "edge detectors". We present here the morphological framework of gradient operators.

The most popular gradients are based on linear transformations and template-matching: Prewitt [19], Sobel [29], Hueckel [8,9], Compass [22,17], Kirsch [10]... For surveys of these techniques, see [5,18]. Generalizations to non-linear edge detectors have been carried out by Roberts [21], Lee and Haralick [13], and Rosenfeld [23,24].

There are many gradients and all of these are potentially useful. From our point of view, this situation comes from four facts: first, the concept of gradient is defined on a continuous basis. The problem is that digital image analysis is done on a discrete basis, resulting in many different approximations. Second, gradients enhance high-frequency events in images. These events may be caused by edges, but are generally caused by noise. We have to improve the S/N ratio before applying such a detector. Compromises have to be made, leading to different types of optimization depending on a particular application. Third, the idea of "real" edges is somewhat fuzzy: picture edges are not necessarily at object boundaries. A canonical definition of an edge is still to be found, if it exists. The fourth and last reason for the proliferation of edge detectors is caused by a lack of performance metrics. There are many criteria of performance, some qualitative, some quantitative. We discuss briefly this problem in section 5.

The last step of an edge detection technique consists in finding the enhanced edges in order to obtain an edge map. Edge maps are generally determined by thresholding the gradient image. There exist however some algorithms based on heuristic search [15,14]. It gives better results, but the heuristics and cost functions and starting points and stop criteria have to be defined with care. These parameters vary from an application to another and may be difficult to set. Mathematical morphology has a powerful edge finder: the watershed transformation [4,3,1,32,28]. With this transformation, detected edges are always connected and thin since they are defined as the boundaries of the catchment basins of the minima of the image gradients.

Section 2 presents the morphological framework needed to define a gradient operator. The basic morphological gradient or Beucher's gradient is detailed in section 3. Section 4 is devoted to other classes of morphological gradients: half gradients, thick gradients, the regularized gradient, directional gradients, thinning/thickening gradients. Applicability and performances of each of these gradients are studied in section 5. Before concluding, section 6 shows how morphological gradients can be generalized to other digital spaces such as those defined by graphs, multidimensional images and vectorial spaces.

# 2 Definitions

Morphological gradients are operators enhancing variations of pixel intensity in a given neighbourhood. In order to do this, we use three different combinations of operators:

- Arithmetic difference between an extensive operator $\phi$ and an anti-extensive operator $\psi$: $\phi(f) - \psi(f)$.
- Arithmetic difference between an extensive operator $\phi$ and the original function $f$: $\phi(f) - f$.
- Arithmetic difference between the original function $f$ and an anti-extensive operator $\psi$: $f - \psi(f)$.

An operator $\phi$ is said to be *extensive* if and only if:

$$f < \phi(f), \forall f. \tag{1}$$

By duality, $\psi$ is *anti-extensive* if and only if:

$$\psi(f) < f, \forall f. \tag{2}$$

# 3 Basic Morphological Gradient of Beucher Gradient

We provide the definition of the morphological gradient for functions defined on the continuous plane. We show that it corresponds to the gradient modulus of the gradient as defined for differentiable functions. We then provide its implementation for discrete images.

## 3.1 Continuous case

Let $f$ be a differentiable function defined on the Euclidean plane $\mathbb{R}^2$. By definition the *gradient* $\nabla$ associated to $f$ is the 2D vector of its partial derivatives in two orthogonal directions $x_1$ and $x_2$:

$$\nabla f = (\frac{\partial f}{\partial x_1}, \frac{\partial f}{\partial x_2}). \tag{3}$$

In the field of image processing, gradients are handled through their modulus and azimuth representations rather than through their vector representation. The gradient modulus is thus:

$$|\nabla f| = \sqrt{(\frac{\partial f}{\partial x})^2 + (\frac{\partial f}{\partial y})^2}. \tag{4}$$

The azimuth or direction *dir* of the gradient is:

$$dir(f) = \arctan[(\frac{\partial f}{\partial x_2})/(\frac{\partial f}{\partial x_1})]. \tag{5}$$

The azimuth corresponds also to the direction which maximizes the first directional derivative. If the directional derivatives are equal to zero for all directions $\theta$ the gradient azimuth is not defined. These definitions hold for continuous spaces but they cannot be directly applied to discrete images defined on a subset of the discrete plane $\mathbb{Z}^2$. This partly explains the variety of gradients for discrete spaces as we pointed out in the introduction. We now give the definition of the morphological gradient in the continuous space $\mathbb{R}^2$.

Let $f$ a function defined on $\mathbb{R}^2$ and $\rho B$ a disk of radius $\rho$. The morphological gradient $g$ of $f$ is defined as follows:

$$g(f) = \lim_{\rho \to 0} \frac{\delta_{\rho B}(f) - \epsilon_{\rho B}(f)}{2\rho}, \tag{6}$$

where $\delta_{\rho B}(f)$ and $\epsilon_{\rho B}(f)$ are respectively the dilation and the erosion [25] of $f$ with a disk $B$ of radius $\rho$. The morphological gradient is always positive as dilations and erosions — with structuring elements containing their origin — are respectively extensive and anti-extensive operations. This gradient is often called Beucher gradient [2].

If $f$ is differentiable, its morphological gradient corresponds to its gradient modulus as defined in Eq. 4. From Fig. 1, it is clear that we can express the erosion and dilation of $f$ at point $x$ in the following way:

$$\delta_{\rho B} f(x) = \sup_{y \in \rho B_x} f(y) = f(x) + \rho |\nabla f(x)| + \rho \nu(\rho), \tag{7}$$

$$\epsilon_{\rho B} f(x) = \inf_{y \in \rho B_x} f(y) = f(x) - \rho |\nabla f(x)| + \rho \nu'(\rho). \tag{8}$$

$\nu$ and $\nu'$ being error terms tending to zero with $\rho$. We have therefore:

$$\delta_{\rho B} f(x) - \epsilon_{\rho B} f(x) = 2\rho |\nabla f(x)| + (\nu(\rho) - \nu'(\rho)). \tag{9}$$

By neglecting the error term for $\rho$ tending to zero, we find:

$$g(x) = |\nabla f(x)|, \text{ Q.E.D.} \tag{10}$$

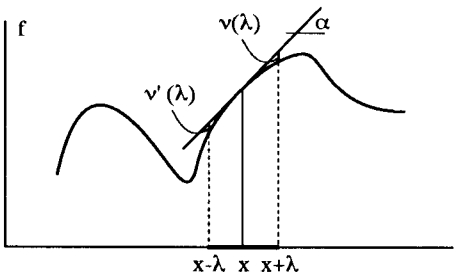


Figure 1: Graph of a 1d function $f$ and its values along a segment of length $2\rho$ centered at $x$. Note that $\tan(\alpha)$ equals to $|\nabla f(x)|$. This figure can be generalized to 2D functions by taking a disk of radius $\rho B$ as structuring element.

### 3.2 Discrete case

Equation 6 applies directly to the discrete case but we do not have access to the limit $\rho \to 0$. The smallest $\rho$ accessible for a digital grid is 1. The morphological gradient in the discrete case was therefore defined by Beucher [2] has the arithmetic difference between the dilated and the eroded of the image with the elementary structuring element $B$ of the considered grid:

$$g(f) = \delta_B(f) - \epsilon_B(f). \tag{11}$$

A discrete morphological gradient on a road scene is shown in Fig. 2.

In Eq. 11, the denominator disappeared because it is now a constant which equals 2. It should be noted that for finite structuring elements this constant does not directly correspond to a distance: the minimum and maximum values are not necessarily separated by the diameter of the neighbourhood. This distance can only be estimated using statistical models of images — if they are available. $g(f)$ represents therefore the maximum variation of the grey level intensities within an elementary neighbourhood rather than an local slope.

## 4 Other Morphological Gradients

### 4.1 Internal and external gradients

In digital images, the thickness of a contour is at least one pixel wide. Moreover, there are differences between external and internal boundaries of a region. This results in gradient thickness of two pixels even for sharp transitions as illustrated in Fig. 3b. Internal and external morphological gradients where tailored to output one-thickness gradients for sharp transitions.

The internal gradient $g^-$ is defined as the difference between the original image and the eroded image:

$$g^-(f) = f - \epsilon_B(f). \tag{12}$$

The internal gradient enhances internal boundaries of white objects. For binary images, the internal gradient will provide a mask of the internal boundaries of the objects of the image.

The external gradient $g^+$ is defined as the difference between the dilated image and the original image:

$$g^+(f) = \delta_B(f) - f. \tag{13}$$

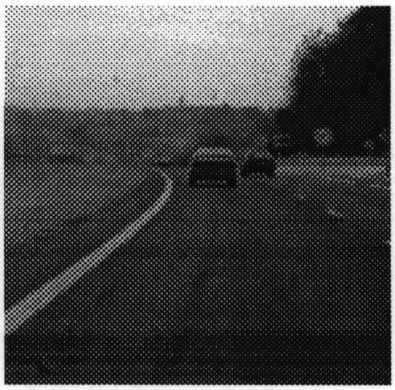

(a) Original image $I$.

(b) Dilated $\delta_B(I)$.

(c) Eroded $\epsilon_B(I)$.

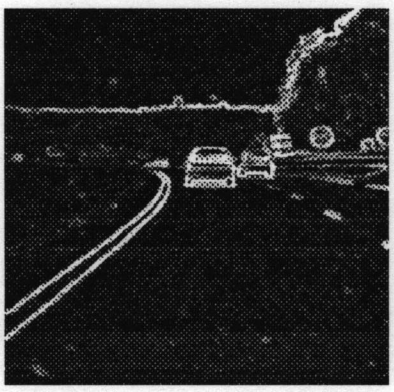

(d) Morphological gradient $g(I) = \delta_B(I) - \epsilon_B(I)$.

Figure 2: Morphological gradient on a road scene.

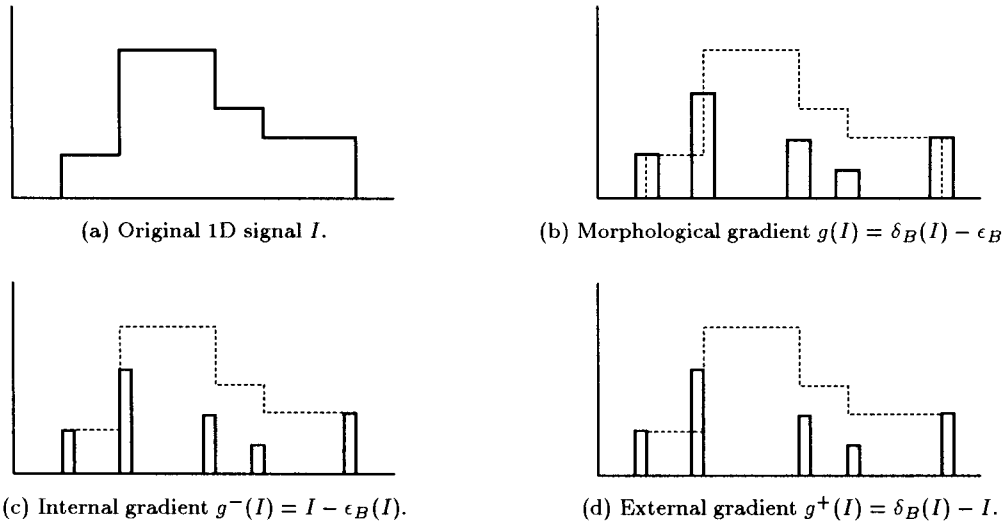

(a) Original 1D signal $I$.

(b) Morphological gradient $g(I) = \delta_B(I) - \epsilon_B(I)$.

(c) Internal gradient $g^-(I) = I - \epsilon_B(I)$.

(d) External gradient $g^+(I) = \delta_B(I) - I$.

Figure 3: Morphological gradients on a 1D digital signal with sharp transitions between homogeneous regions.

The external gradient extracts external boundaries of white objects. In Fig. 3, internal and external gradients are compared to the morphological gradient.

Internal and external gradients are sometimes called "half gradients". They are used when thin contours are needed. The choice between internal or external gradient depends on the nature of the objects to be extracted. For instance, an external gradient applied on a thin dark structure will provide a thin edge whereas an internal gradient will give a double edge.

## 4.2 'Thick' gradients

The discrete morphological gradient is defined on basic morphological operations with an elementary structuring element ($\rho = 1$). Thick gradients $g_\rho$ are defined with structuring elements of size $\rho > 1$.

$$g_\rho(f) = \delta_{\rho B}(f) - \epsilon_{\rho B}(f). \tag{14}$$

An example of thick gradient is provided in Fig. 4. Thick gradients give the maximum variation of the function in a neighbourhood of size $\rho$. If the size $\rho$ is tuned in order to correspond to the width $e$ of the transition between regions of homogeneous grey level, the thick gradient will give the step grey level difference $h$ between these regions (see Fig. 5). Thick gradients are at the basis of the definition of the regularized gradient presented in the next section.

## 4.3 Regularized gradient

Thick gradients allow to determine grey level steps between homogeneous regions. Thick gradients have however numerous drawbacks. First they are parametric since the size $\rho$ must be determined. Generally this size is unknown and, even worse, is not necessarily constant all over the image frame. Second, resulting edges are thick and classical edge finding techniques are not well suited for such

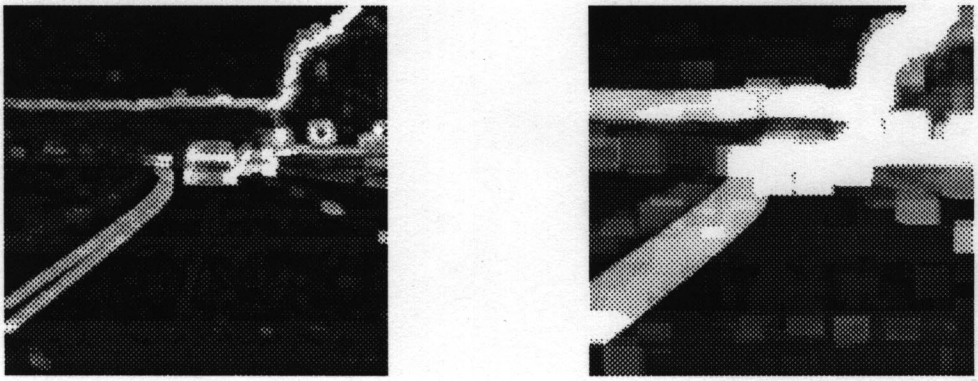

(a) $g_3(I)$. (b) $g_{10}(I)$.

Figure 4: Thick gradients on the image $I$ of Fig. 2a.

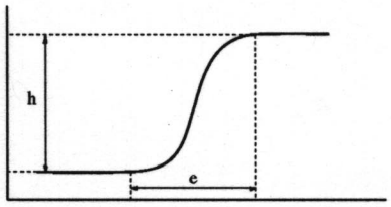


Figure 5: Profile of the grey levels along the transition between two homogeneous regions.

contours. Finally, homogeneous regions narrower than $2\rho$ cannot be segmented with thick gradients. Beucher [2] proposed a regularized gradient avoiding these drawbacks.

The thickness of contours resulting from a thick gradient of size $\rho$ can be reduced by eroding the thick gradient with the disk of size $\rho - 1$:

$$\epsilon_{(\rho-1)B}[g_\rho(f)]. \tag{15}$$

The erosion does not allow to recover contours of regions narrower than $2\rho$. Indeed, the gradients coming from the boundaries of these regions merge and the subsequent erosion will not split them back (see Fig. 6 and the two parallel white lines in Fig. 4b). This will cause artefacts in the contour detection step. We propose now a solution to solve this problem. When thick gradients coming from two distinct boundaries merge, the resulting thickness is larger than $2\rho$. These regions can be extracted by a morphological top hat of size $\rho$. The white top hat transform WTH [16] of a

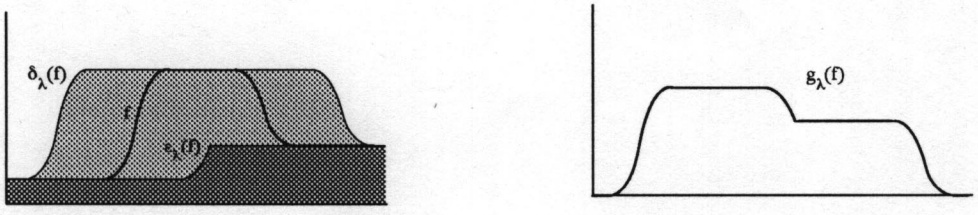


(a) Original 1D signal $f$ and its eroded and dilated. (b) Thick gradient of $f$: $g_\rho(f) = \delta_{\rho B}(f) - \epsilon_{\rho B}(f)$.

Figure 6: Thick gradient: contour coming from edge A and B have merged.

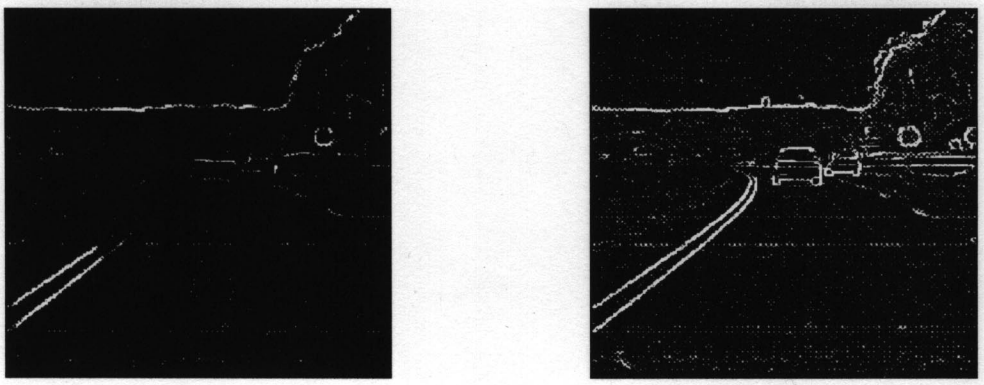

(a) $g_3^\star(I)$.

(b) $g^\star(I)$.

Figure 7: Regularized gradients on the road scene $I$ of Fig. 2.

function $f$ is defined as the difference of the function with its morphological opening $\gamma$ of size $\rho$:

$$WTH_\rho(f) = f - \gamma_\rho(f). \tag{16}$$

The white top hat transformation extracts all bright image regions smaller than $2\rho$. A white top hat transform can therefore be applied on thick gradients to remove all regions where the gradients coming from two distinct boundaries have merged. This white top hat transform is followed by an erosion of size $\rho - 1$ to give a thin gradient $g_\rho^\star$ called the parametric regularized gradient of size $\rho$:

$$g_\rho^\star(f) = \epsilon_{(\rho-1)B}(WTH_\rho[g_\rho(f)]). \tag{17}$$

By using $g_\rho^\star$, regions larger than $2\rho$ are well delineated. The top hat transform has removed all gradients coming from regions narrower than $2\rho$. Consequently, their contours will not appear in $g_\rho^\star$. For a transition of width $e$ as shown in 5, $g_\rho^\star$ will give a gradient proportional to $h$ if $\rho$ is greater to $e$ (until the size of the contoured is exceeded). When applied for all sizes $\rho$, $g_\rho^\star$ allows to determine the thickness of each contour as well as the width of the contoured objects. These two parameters can be used to organize the contours into a hierarchy. To have an edge map for all scales, the supremum between the $g_\rho^\star$ for all possible $\rho$ must be considered:

$$g^\star(f) = \sup_\rho [g_\rho^\star(f)]. \tag{18}$$

$g^\star$ is called the non-parametric regularized gradient [2]. Examples of regularized gradients are shown in Fig. 7.

## 4.4 Directional gradients

Directional gradients are defined using linear structuring elements. These gradients exhibit sensivity to different directions in images [11]. We can extract from them the modulus and the azimuth.

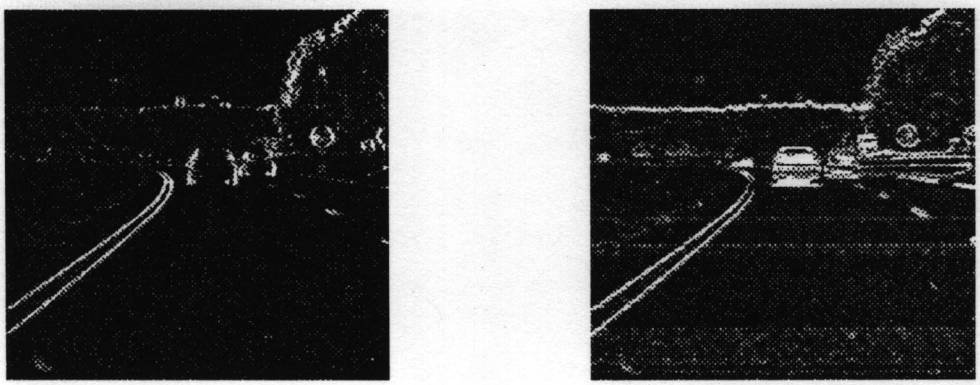

(a) Horizontal direction.

(b) Vertical direction.

Figure 8: Directional gradients of image $I$ of Fig. 2a.

### 4.4.1 Modulus

Beucher's gradient defined in equation 6 can be redefined with linear structuring elements $L$ along direction $\alpha$:

$$g^{\alpha} = \delta_{L^{\alpha}}(f) - \epsilon_{L^{\alpha}}(f), \tag{19}$$

On digital grids, the number of available directions is finite; on a square grid, it is 2 or 4, depending if we use the block distance or the chessboard distance. On a hexagonal grid, there are three possible directions. Morphological directional gradients are illustrated in Fig. 8.

The internal directional gradient $g^{-,\alpha}$ and external directional gradient $g^{+,\alpha}$ are defined in the same way as internal and external gradients:

$$g^{-,\alpha}(f) = f - \epsilon_{L^{\alpha}}(f), \tag{20}$$

$$g^{+,\alpha}(f) = \delta_{L^{\alpha}}(f) - f. \tag{21}$$

We may also use "thick" directional gradients of thickness $\rho$, by taking $\rho L$ instead of $L$ as linear structuring element. In this case, the number of available directions increases at the expense of operator resolution.

### 4.4.2 Azimuth

There are two ways to define the azimuth of the gradient. The first corresponds to the arc tangeant of the directional gradient in the horizontal direction $x$ divided by the directional gradient in the vertical direction $y$:

$$dir(g) = \arctan(g^x/g^y). \tag{22}$$

The other definition is more grid-dependent. It works by computing the gradient modulus in all grid directions. The direction maximizing the gradient modulus will be assigned to the output. There may be problems when the maximum gradient is defined for more than one direction. Some decision rules must be devised in order to remove ambiguities:

- Non-adjacent directions on the grid cancel out each other.

- The remaining adjacent directions are averaged. This will generate directions between pixels without increasing the size of the neighbourhood.

### 4.5 Thinning and thickening gradients

Thickenings and thinnings are extensive and anti-extensive operators respectively. There are the basic operators for a gradient definition. Thinnings and thickenings on functions are defined [25, page 450] in terms of dilations and erosions. The operations are done with composite structuring elements $T = (T_1, T_2)$. The thickening $\bullet$ of $f$ with $T$ is defined:

$$f \bullet T_\alpha = \begin{cases} \epsilon_{T_1}(f) & \text{if } \delta_{T_2}(f) < f \leq \epsilon_{T_1}(f) \\ f & \text{otherwise.} \end{cases} \tag{23}$$

Similarly, the thinning $\circ$ of $f$ with $T$ is defined:

$$f \circ T_\alpha = \begin{cases} \delta_{T_2}(f) & \text{if } \delta_{T_2}(f) < f \leq \epsilon_{T_1}(f) \\ f & \text{otherwise.} \end{cases} \tag{24}$$

The only useful thinnings/thickenings gradients use directional structuring elements $T_\alpha$ in the following way:

$$(f \bullet T_\alpha) - (f \circ T_\alpha). \tag{25}$$

Internal and external gradients can also be defined using the same principles as shown in section 4.1 but are of limited use.

## 5 Comparing Morphological Gradients

Fram and Deutsch's [6] experiment is the prototype of gradient evaluation: an artificial image containing "ideal" edges, and corrupted with increasing amounts of noise. There are questions associated with this kind of approach: does the test image reflects the reality? Did the "true edges" move because of the noise?

There are very few theoretical arguments in favor of a given gradient. This is because theoretical comparisons generally use approximations too crude as compared to real cases. There are mostly qualitative reasons to choose a particular operator. In this section, we summarize some rules an expert would use when choosing an operator according to varying aims:

- Noise sensitivity.
- Fine details loss: compromises have to be made in order to have a low noise sensitivity and conservation of fine details.
- Thin result: It is an important criterion for searching algorithms and thresholdings, less for watersheds –the divide lines will be at the geometrical center of plateaus forming crestlines.
- Directional information: it depends on an application.
- Black/white symmetry: this criterion comes from the fact that morphological operators behave asymetrically on image maxima and minima. For instance, external gradients $g^+$ will displace the "edge" to the exterior of a bright object. Fig. 3d illustrates this example.

| Gradient | noise | details | thinness | direct. | symmet. | parametric | load |
|---|---|---|---|---|---|---|---|
| Beucher | med | med | med | no | yes | no | low |
| half gradients | med | small | high | no | no | no | very low |
| thick | low | large | low | no | yes | yes | med |
| regularized | low | med | high | no | yes | no | very high |
| directional | med | med | med | yes | yes | yes | med |
| thin/thick | high | small | high | yes | yes | no | high |

Table 1: Qualitative comparison of morphological gradients according to various criteria.

- Parametric: if some *a priori* knowledge is available, it is possible to use gradients having intrinsic parameters. These concern the shape and size of the structuring elements constructing the operator.

- Computational load: the choice of gradients is often limited by the computational load they demand, in particular in real-time applications.

The most frequently used morphological gradient is the Beucher gradient. It is a general-purpose gradient with good properties of symmetry and a good compromise between thinness and noise immunity. However, in some applications the result may be too thick and thinner gradients must be used. Thinning/thickening gradients may be used in such a situation. Half gradients may be useful because of their thinness and their relative noise immunity. However, they tend to displace contours, enlarging bright objects for the external gradient and shrinking them for the internal gradient. This artefact is easy to correct if the intensity of the objects to be contoured with respect to the background is known. The regularized gradient creates a hierarchy by using a multiscale approach. The detected contour intensities will depend on the size and the constrast of the regions on the original image. Significant objects will be retained regardless of their size.

# 6 Gradients in Other Digital Spaces

All previous sections were dealing with 2D grey level images. We now propose morphological gradients in some other digital spaces.

## 6.1 Multidimensional

Images under study are here defined on subsets of $\mathbb{Z}^n$. All morphological gradients defined for 2D images apply to $n$D images. One has just to consider the appropriate structuring element. For example, Beucher gradient on a 3D image is computed with the approximation of the sphere in the considered grid. One must however take care of the dimensionality [27,20] of such an operator. Indeed, if the units of the image space are not homogeneous it is of little physical meaning to compute a gradient. For instance this is the case for 3D images coming from a temporal series of 2D images. Here, only directional gradients along the temporal axis or along the 2D image plane are allowed.

## 6.2 Graphs

A graph consists of a set of nodes linked by a set of vertices. It has already been demonstrated that morphological operators extend to general graphs [26,30,31]. Beucher gradient, half gradient, and regularized gradient are therefore suited for computing gradient on graphs. However, directional and thinnings/thickenings operators are not defined on general graphs and morphological gradients based on these operators do not extend to this lattice; directional information and shape information are generally not available from a general graph.

## 6.3 Multispectral and textural

Multispectral images constitute a lattice where a vector —or a function— of grey level values is defined for each pixel. This constrasts with a grey-level image where a pixel has a single value. Morphological operators exist on this lattice. Dilations and erosions are performed on each vector component separately.

There are many ways to define gradient operators on this lattice. Di Zenzo [34] determined gradient modulus for each vector component and combined them using different distances. Lee and Cox [12] considered multispectral images as vector fields and defined a gradient modulus from the matrix of its partial derivatives

Morphological gradients are constructed with the morphological operators the same way as in section 3. We have the same problem as Di Zenzo had in order to calculate the modulus: we must combine the different vector components. This is done by computing distances. There is a great choice of distances. The most frequently used distance is the Euclidean distance.

Texture descriptors extract statistical or structural [7,33,35] information from a pixel neighbourhood. There are presently three approaches to image segmentation: thresholding, edge detection and region detection. In texture segmentation the contour detection approach is rarely used. This approach makes use of multispectral gradients.

We propose to use textural descriptors to generate vectorial images. A descriptor is generally applied over regions in images. In this approach, we apply them on sliding windows. The center of such windows is a textural vector. Edge-oriented texture segmentation can be achieved with vectorial gradients.

Figure 9 illustrates this. The original image has two regions of same average value. Only orientation is different. We used for texture descriptors the average output of directional openings in a square sliding window. We performed edge detection with Beucher gradient $g_i(f)$ on each component separately. The modulus was calculated with the Euclidean distance: $\sqrt{\sum_i^n (g_i(f))^2}$. After gradient modulus filtering, we performed a watershed transformation, giving the segmented image in the figure 9.

# 7 Conclusion

Object boundaries are often characterized by grey-level intensity transitions. In order to detect these variations, gradient masks are widely used. The morphological approach to gradients consists in determining a grey level variation within a given neighbourhood using extensive and anti-extensive operators. A menagery of morphological gradients have been presented, each gradient corresponding to a particular model of grey level transitions along object boundaries. The applicability of

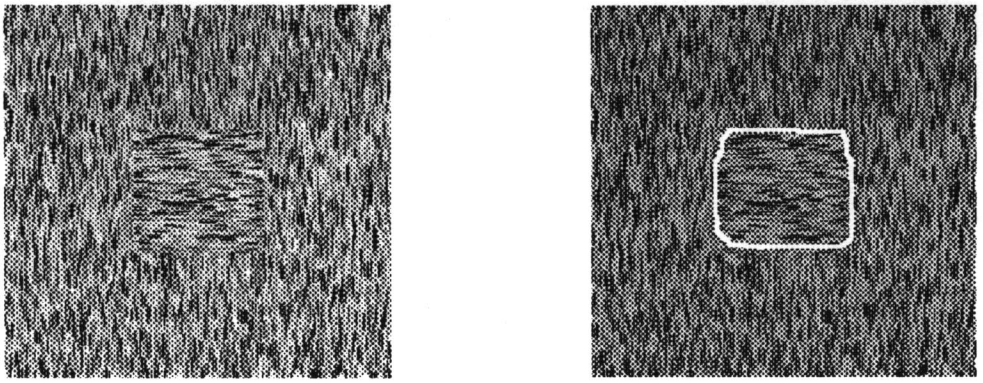

(a) Original image. (b) Segmented image.

Figure 9: Texture segmentation using vector gradients.

all these gradients have been evaluated. Morphological gradients are not necessarily better than other gradients. The performances of a gradient depend on an application and must be tested on it. Morphological gradients should therefore be considered as a possible alternative to classical gradients.

# References


[1] Serge Beucher. Watersheds of functions and picture segmentation. In *ICASSP 82, Proceedings IEEE International Conference on Acoustics, Speech and Signal Processing, Paris*, pages 1928–1931, May 1982.

[2] Serge Beucher. *Segmentation d'images et morphologie mathématique.* PhD thesis, Ecole des Mines de Paris, June 1990.

[3] Serge Beucher. Segmentation tools in mathematical morphology. Technical Report No. N-32/90/MM, Centre de Morphologie Mathématique, Ecole des Mines de Paris, 1990.

[4] Serge Beucher and C. Lantuéjoul. Use of watersheds in contour detection. In *International Workshop on Image Processing: Real-Time Edge and Motion detection/estimation, Rennes*, September 1979.

[5] L.S. Davis. A survey of edge detection techniques. *Computer Graphics and Image Processing*, 4:248–270, 1975.

[6] J.R. Fram and E.S. Deutsch. On the quantitative evaluation of edge detection schemes and their comparison with human performance. *IEEE Transactions on Computers*, C-24(6):616–628, 1975.

[7] Robert M. Haralick. Statistical and structural approaches to texture. *Proceedings of the IEEE*, 67(5):786–804, May 1979.

[8] Manfred H. Hueckel. An operator which locates edges in digitized pictures. *Journal of the Association for Computing Machinery*, 18(1):113–125, January 1971.

[9] M.H. Hueckel. An operator which locates edges in digital pictures. *J. Assoc. Comput. Mach.*, 18:113–125, January 1971.

[10] R. Kirsch. Computer determination of the constituent structure of biological images. *Computers and Biomedical Research*, 4:315–328, 1971.

[11] Mohamad Bassam Kurdy. *Transformations morphologiques directionnelles et adaptatives: applications aux sciences des matériaux.* PhD thesis, Ecole des Mines de Paris, September 1990.

[12] Hsien-Che Lee and David R. Cok. Detecting boundaries in a vector field. *IEEE Transactions on Signal Processing*, 39(5):1181–1194, May 1991.

[13] James S. J. Lee, Robert M. Haralick, and Linda G. Shapiro. Morphologic edge detection. In *8th Int. Conf. Pattern Recognition, Paris*, pages 369–373, 1986.

[14] J. Lester, H. Williams, B. Weintraub, and J. Brenner. Two graph searching techniques for boundary finding in white blood cell images. *Comput. Bio. Med.*, 8:293–308, 1978.

[15] A. Martelli. Edge detection using heuristic search methods. *Computer vision, Graphics, and Image Processing*, 1:335–345, 1971.

[16] F. Meyer. *Cytologie quantitative et morphologie mathématique.* PhD thesis, Ecole des Mines de Paris, 1979.

[17] R. Nevatia and K.R. Babu. Linear feature extraction and description. *Computer Vision, Graphics, and Image Processing*, 13:257–269, 1980.

[18] T. Peli and D. Malah. A study of edge detection algorithms. *Computer Graphics and Image Processing,*, 20:1–21, 1982.

[19] J.M.S. Prewitt. Object enhancement and extraction. In B. Lipkin and Azriel Rosenfeld, editors, *Picture Processing and Psychopictorics*, pages 75–149, New York, 1970. Academic Press.

[20] J.-F. Rivest, J. Serra, and P. Soille. Dimensionality and image analysis. *Journal of Visual Communication and Image Representation*, 1991.

[21] L.G. Roberts. Machine perception of three-dimensional solids. In J. T. Trippett and al., editors, *Optical and Electrooptical Information Processing*, pages 159–197, Cambridge, 1965. MIT Press.

[22] G.S. Robinson. Edge detection by compass gradient masks. *Computer Vision, Graphics, and Image Processing*, 6:492–501, 1977.

[23] Azriel Rosenfeld and M. Thurston. Edge and curve detection for visual scene analysis. *IEEE Transactions on Computers*, C-20:562–569, 1971.

[24] Azriel Rosenfeld, M. Thurston, and Y.H. Lee. Edge and curve detection: Further experiments. *IEEE Transactions on Computers*, C-21:677–715, 1972.

[25] Jean Serra. *Image Analysis and Mathematical Morphology.* Academic Press London, 1982.

[26] Jean Serra, editor. *Image Analysis and Mathematical Morphology - Theorical Advances.* Academic Press, London, 1988.

[27] P. Soille, J.-F. Rivest, and J. Serra. Dimensionality and image analysis. In *SPIE IS&T 1992 Symposium on Electronic Imaging: Science and Technology.* SPIE, February 1992.

[28] Pierre Soille and Luc Vincent. Determining watersheds in digital pictures via flooding simulations. In *SPIE Visual Communications and Image Processing '90 Lausanne.*, volume 1360, 1990.

[29] J.M. Tennenbaum, A.C. Kay, T. Binford, G. Falk, J. Feldman, G. Grape, R. Pau, K. Pingle, and I. Sobel. The sobel edge detector. In D.A. Walker and L.M. Norton, editors, *Proceedings. I.J.C.A.I.*, 1969.

[30] L. Vincent. Graphs and mathematical morphology. *Signal Processing*, 16:365–388, 1989.

[31] Luc Vincent. *Algorithmes morphologiques à base de files d'attente et de lacets. Extension aux graphes.* PhD thesis, Ecole des Mines de Paris, May 1990.

[32] Luc Vincent and Pierre Soille. Watersheds in digital spaces: An efficient algorithm based on immersion simulations. *IEEE Transactions on Pattern Analysis and Machine Intelligence*, 13(6):583–598, June 1991.

[33] Harry Wechsler. Texture analysis - a survey. *Signal Processing*, 2:271–282, 1980.

[34] S. Di Zenzo. A note on the gradient of a multi-image. *Computer Vision, Graphics and Images Processing*, 33:116–125, 1986.

[35] Steven W. Zucker. Toward a model of texture. *Computer Graphics and Image Processing*, 5:190–202, 1976.